Proceedings of the 1997 IEEE
International Conference on Robotics and Automation
Albuquerque, New Mexico - April 1997

Analysis of A 5-bar Finger Mechanism Having Redundant Actuators With Applications to Stiffness and Frequency Modulations

Byung-Ju Yi[1], Il Hong Suh[2], Sang-Rok Oh[3]

[1]Dept. of Control and Instrumentation Eng., Hanyang Univ. Korea
[2]Dept. of Electronics Eng., Hanyang Univ. Korea
[3]Dept. of Electronics and Information Tech. KIST, Korea
Email : bj@hyunp1.hanyang.ac.kr

Abstract

For a 5-bar finger mechanism with redundant actuators, it is shown that judicial choice of the location of one redundant actuator greatly enhances the load handling capacity of the system, when compared to that of nonredundant systems. And, it is also shown that excessive redundant actuation enables the system to modulate the end-point stiffness or motion frequency by internal load distributions. Especially, the motion frequency modulation via internal loads in redundantly actuated closed-chain systems is believed to be fairly new. To show the effectiveness of the proposed algorithms, several simulation results are illustrated.

I. Introduction

Mobility of a system is defined as the number of independent variables which must be specified in order to locate its elements relative to another. It is described by

$$D = N(L-1) - \sum_{i=1}^{J} (N-F_i) \qquad (1)$$

where N, L, and F_i denote the degree-of-freedom of the operational (or task) space, the number of links, and the motion degree-of-freedom of the ith joint, respectively.

When D is greater than N, the system is called *a kinematically redundant system*. On the other hand, when the number of actuators is greater than D (this situation usually happens in a closed-chain system), the system is called *a redundantly actuated system*. General biomechanical systems including the Human body as well as the bodies of mammals and insects are redundantly actuated. For example, Mobility of the Human upper-extremity (arm) can be considered as 7, while it has 29 human actuators (i.e, muscles). Accordingly, it has 22 redundant actuators. Redundant actuation can be also found in many robotic applications[3-5]. They include multiple arms, dual arms, multi-fingered hands, walking machines.

Our work will be focused on useful applications of redundant actuation. Specifically for a 5-bar finger mechanism with redundant actuators, it is shown that one additional redundant actuator greatly enhances the load handling capacity of the system. The actuator location should be carefully decided to maximize the performance enhancement. And, it is also shown that excessive redundant actuation enables the system to modulate the end-point stiffness or motion frequency by internal load distributions. Especially, the motion frequency modulation via internal loads in redundantly actuated closed-chain systems is believed to be fairly new.

The organization of this paper is as follows : Initially, we introduce the kinematic and dynamic modeling methodology in section 2. In section 3, enhancement of maximum load handling capacity is shown to be possible when using redundant actuation. Stiffness and frequency modulation algorithm will be proposed in section 4. Simulation results are included in sections 3 and 4 to corroborate our proposed concepts. Finally, we draw conclusions.

2. Kinematic Modeling

The modeling methodology integrates the Generalized Principle of D'Alembert with the method of kinematic influence coefficients(KIC) resulting in closed form vector expressions. The reader is referred to Freeman and Tesar [6] for a more detailed description. In the following the letters G and H stand for 1*st* and 2*nd* order KIC matrices, respectively, and superscribed quantities indicate dependent parameters while subscripts denote the independent parameters.

2.1 Open-chain kinematics

Assume that a closed-chain mechanism consists of R chains. Adopting the standard Jacobian representation for the velocity of a vector of N dependent (output) parameters u in terms of a set of M independent input coordinates ${}_r\dot{\phi}$ of r*th* open-chain, one has

$$\dot{u} = [\,{}_rG^u_\phi\,]\;{}_r\dot{\phi}\,, \qquad (2)$$

where the Jacobian $[\,{}_rG^u_\phi\,]$ with dimension $N\times M$ relates the coordinates u and ${}_r\dot{\phi}$. Generally, the acceleration vector $\ddot{u}$ of a set of N dependent parameters u is represented in terms of the M independent coordinates ϕ as

$$\ddot{u} = [\,{}_rG^u_\phi\,]\;{}_r\ddot{\phi} + {}_r\dot{\phi}^T[\,{}_rH^u_{\phi\phi}\,]\;{}_r\dot{\phi}, \qquad (3)$$

where the second-order KIC array $[\,{}_rH^u_{\phi\phi}\,]$ is of dimension of $N\times M\times M$, and the *ith* plane of $[\,{}_rH^u_{\phi\phi}\,]$,

$[{}_rH^u_{\phi\phi}]_i$, with dimension of $M\times M$ is defined as

$$[{}_rH^u_{\phi\phi}]_i = \left[\frac{\partial^2 u_i}{\partial_r\phi\,\partial_r\phi}\right] = \begin{bmatrix} h^{u_i}_{\phi_1\phi_1} & h^{u_i}_{\phi_1\phi_2} & \cdots & h^{u_i}_{\phi_1\phi_N} \\ h^{u_i}_{\phi_2\phi_1} & h^{u_i}_{\phi_2\phi_2} & \cdots & h^{u_i}_{\phi_2\phi_N} \\ \vdots & & \vdots & \\ h^{u_i}_{\phi_N\phi_1} & h^{u_i}_{\phi_N\phi_2} & \cdots & h^{u_i}_{\phi_N\phi_N} \end{bmatrix}. \quad (4)$$

2.2 Internal kinematics for 5-bar Finger mechanism

Consider a 5-bar finger mechanism shown in Fig. 1. This system has two typical features. As the first feature, it has one closed-kinematic chain. The closed-kinematic chain is formed by connecting the two open-chains at the given location of the second link of the left open-chain, as shown in Fig. 1. In order to enlarge the area encompassed by the finger, the folded-in configuration of the right open-chain is chosen. As the second feature, there exist several choices in the selection of independent joints (i.e., actuator locations). Since Mobility of this mechanism is two, two actuators are minimally required to control the mechanism. In general, the base joints have been chosen as the actuator locations in previously developed 5-bar systems [7], primarily to minimize the dynamic effect due to floating actuators. However, from a kinematic point of view, inclusion of one or two floating actuators may be a better choice. For example, a better manipulability, isotropy, or load handling capacity can be achieved by using a certain floating actuator. An internal kinematic relationship between the dependent joints and the independent joints is required to deal with the problem addressed in the above.

The two open-chain of the 5-bar mechanism have a common kinematic relation at the end-point of the system. Suppose that the end-point vector of the 5-bar is denoted as $\boldsymbol{u} = (x\ y\ \Phi)^T$, then the components of $\boldsymbol{u}$ is described by

$$x = l_1c_1 + l_2c_{12} = a + l_3c_3 + l_4c_{34} + l_5c_{345}, \quad (5)$$

$$y = l_1s_1 + l_2s_{12} = l_3s_3 + l_4s_{34} + l_5s_{345}, \quad (6)$$

and

$$\Phi = \theta_1 + \theta_2 = \theta_3 + \theta_4 + \theta_5. \quad (7)$$

Also, the equivalent velocity and acceleration relations are, respectively, given by

$$\dot{\boldsymbol{u}} = [{}_1G^u_\theta]_1\,\dot{\boldsymbol{\theta}} = [{}_2G^u_\theta]_2\,\dot{\boldsymbol{\theta}} \quad (8)$$

$$\ddot{\boldsymbol{u}} = [{}_1G^u_\theta]_1\,\ddot{\boldsymbol{\theta}} + {}_1\dot{\boldsymbol{\theta}}^T[{}_1H^u_{\theta\theta}]_1\,\dot{\boldsymbol{\theta}} = [{}_2G^u_\theta]_2\,\ddot{\boldsymbol{\theta}} + {}_2\dot{\boldsymbol{\theta}}^T[{}_2H^u_{\theta\theta}]_2\,\dot{\boldsymbol{\theta}} \quad (9)$$

where $[{}_1G^u_\theta]$ and $[{}_2G^u_\theta]$ representing the Jacobians of the first and second open-chain are given by

$$[{}_1G^u_\theta] = \begin{bmatrix} -(l_1s_1 + l_2s_{12}) & -(l_2s_{12}) \\ (l_1c_1 + l_2c_{12}) & (l_2c_{12}) \\ 1 & 1 \end{bmatrix} \quad (10)$$

and

$$[{}_2G^u_\theta] = \begin{bmatrix} -l_3s_3 - l_4s_{34} - l_5s_{345} & -l_4s_{34} - l_5s_{345} & -l_5s_{345} \\ l_3c_3 + l_4c_{34} + l_5c_{345} & l_4c_{34} + l_5c_{345} & l_5c_{345} \\ 1 & 1 & 1 \end{bmatrix} \quad (11)$$

respectively, and $[{}_1H^u_{\theta\theta}]$ and $[{}_2H^u_{\theta\theta}]$ representing the Hessian arrays of the first and second open-chain of the system are given by

$$[{}_1H^u_{\theta\theta}]_1 = \begin{bmatrix} -(l_1c_1 + l_2c_{12}) & -(l_2c_{12}) \\ -(l_2c_{12}) & -(l_2c_{12}) \end{bmatrix}, \quad (12)$$

$$[{}_1H^u_{\theta\theta}]_2 = \begin{bmatrix} -(l_1s_1 + l_2s_{12}) & -(l_2s_{12}) \\ -(l_2s_{12}) & -(l_2s_{12}) \end{bmatrix}, \quad (13)$$

$$[{}_1H^u_{\theta\theta}]_3 = \begin{bmatrix} 0 & 0 \\ 0 & 0 \end{bmatrix}, \quad (14)$$

$$[{}_2H^u_{\theta\theta}]_1 = \begin{bmatrix} -(l_3c_3 + l_4c_{34} + l_5c_{345}) & -l_4c_{34} - l_5c_{345} & -l_5c_{345} \\ -l_4c_{34} + l_5c_{345} & -l_4c_{34} + l_5c_{345} & -l_5c_{345} \\ -l_5c_{345} & -l_5c_{345} & -l_5c_{345} \end{bmatrix} \quad (15)$$

$$[{}_2H^u_{\theta\theta}]_2 = \begin{bmatrix} -(l_3s_3 + l_4s_{34} + l_5s_{345}) & -l_4s_{34} - l_5s_{345} & -l_5s_{345} \\ -l_4s_{34} - l_5s_{345} & -l_4s_{34} - l_5s_{345} & -l_5s_{345} \\ -l_5s_{345} & -l_5s_{345} & -l_5s_{345} \end{bmatrix} \quad (16)$$

and,

$$[{}_2H^u_{\theta\theta}]_3 = \begin{bmatrix} 0 & 0 & 0 \\ 0 & 0 & 0 \\ 0 & 0 & 0 \end{bmatrix}. \quad (17)$$

Deciding the joints θ_1 and θ_3 as the independent joints ($\boldsymbol{\theta}_a$) and the joints θ_2, θ_4, and θ_5 as the dependent joints ($\boldsymbol{\theta}_p$), Eq. (8) can be rearranged according to the following form

$$[A]\,\dot{\boldsymbol{\theta}}_p = [B]\,\dot{\boldsymbol{\theta}}_a \quad (18)$$

where

$$[A] = [-[{}_1G^u_\theta]_2\ [{}_2G^u_\theta]_{2,3}], \quad (19)$$

$$[B] = [[{}_1G^u_\theta]_1\ -[{}_2G^u_\theta]_1], \quad (20)$$

$$\dot{\boldsymbol{\theta}}_p = (\dot\theta_3\ \ \dot\theta_4\ \ \dot\theta_5)^T, \quad (21)$$

and

$$\dot{\boldsymbol{\theta}}_a = (\dot\theta_1\ \ \dot\theta_2)^T. \quad (22)$$

From Eq. (19), $[{}_1G^u_\theta]_2$ denotes the first column of $[{}_1G^u_\theta]$ and $[{}_2G^u_\theta]_{2,3}$ denotes the second and third column of $[{}_2G^u_\theta]$.

Now, premultiplying the inverse of the matrix [A] to both sides of Eq. (18) yields

$$\dot{\boldsymbol{\theta}}_p = [G^p_a]\,\dot{\boldsymbol{\theta}}_a, \quad (23)$$

where $[G^p_a]$ denotes the first-order KIC matrix relating $\dot{\boldsymbol{\theta}}_p$ to $\dot{\boldsymbol{\theta}}_a$.

The second-order KIC array $[H^p_{aa}]$ relating $\ddot{\boldsymbol{\theta}}_p$ to $\ddot{\boldsymbol{\theta}}_a$ can be easily obtained in a similar manner. The derivation of $[H^p_{aa}]$ is omitted here.

According to the duality existing between the velocity vector and force vector, the force relation between the independent joints and the dependent joints is described by

$$\begin{pmatrix} T_1 \\ T_2 \end{pmatrix} = [G_a^{\phi}]^T \begin{pmatrix} T_3 \\ T_4 \\ T_5 \end{pmatrix}. \quad (24)$$

Then, the effective load referenced to the independent joints is given by

$$T_a^* = T_a + [G_a^{\phi}]^T \begin{pmatrix} T_3 \\ T_4 \\ T_5 \end{pmatrix} = [G_a^{\phi}]^T T_{\phi} \quad (25)$$

where

$$[G_a^{\phi}] = \begin{bmatrix} I \\ [G_a^{\phi}] \end{bmatrix} \quad (26),$$

and

$$T_a = (T_1\ T_2)^T,\ T_{\phi} = (T_1\ T_2\ T_3\ T_4\ T_5)^T. \quad (27)$$

2.3 *Forward Kinematics for 5-bar mechanism*

Since the joints of the *r*th chain is composed of some of the independent and dependent joints, $({}_r\dot{\phi})$ can be expressed in terms of the total system's active(independent) joints by

$${}_r\dot{\phi} = [{}^rG_a^{\phi}]\ \dot{\phi}_a \quad (28)$$

where the matrix $[{}^rG_a^{\phi}]$ is formed using elements of $[G_a^{\phi}]$ augmented with a one in the *ith* row and *jth* column and with zeros in all other elements of the *ith* row if ${}_r\phi_i = \phi_{a_j}$. Thus, the forward kinematics for the common object is obtained by embedding the first-order KIC into one of the *r*th pseudo open-chain kinematic expressions as follows :

$$\dot{u} = [{}_rG_{\phi}^u]\ {}_r\dot{\phi} = [G_a^u]\ \dot{\phi}_a, \quad (29)$$

where the forward Jacobian is determined by

$$[G_a^u] = [{}_rG_{\phi}^u][{}^rG_a^{\phi}]. \quad (30)$$

Using the same augmentation method employed in Eq. (29 evaluation of the second-order forward kinematic array $[H_{aa}^u]$ is also straightforward. It is given by [1]

$$[H_{aa}^u] = [{}_rG_{\phi}^u] \cdot [{}^rH_{aa}^{\phi}] + [{}^rG_a^{\phi}]^T [{}_rH_{\phi\phi}^u][{}^rG_a^{\phi}]. \quad (31)$$

2.4 *Dynamic modeling for 5-bar mechanism*

In this section, we introduce a dynamic model of the 5-bar mechanism consisting of two open kinematic chains. Using the principle of virtual work, the generalized inertial loads of an M-link open-chain as referenced to the M relative joint parameters are given as [6]

$${}_rT_{\phi} = [{}_rI_{\phi\phi}]\ {}_r\ddot{\phi} + {}_r\dot{\phi}^T[{}_rP_{\phi\phi\phi}^*]\ {}_r\dot{\phi},\ r = 1, 2. \quad (32)$$

where the effective inertia matrix and the inertia power array are given by

$$[{}_rI_{\phi\phi}^*] = \sum_{j=1}^{N} ({}_rm_{jk}[{}_rJ_{\phi}^c]^T[{}_rJ_{\phi}^c] + [{}_rG_{\phi}^{jk}]^T[{}_rJ^{jk}][{}_rG_{\phi}^{jk}]) \quad (33)$$

and

$$[{}_rP_{\phi\phi\phi}^*] = \sum_{j=1}^{N} \{ {}_rm_{jk}([{}_rJ_{\phi}^c]^T o [{}_rH_{\phi\phi}^c]) + \quad (34)$$
$$([{}_rG_{\phi}^{jk}]^T[{}_rJ^{jk}]) o [{}_rH_{\phi\phi}^{jk}] + [{}_rG_{\phi}^{jk}]^T([{}_rG_{\phi}^{jk}]^T o [{}_r\Sigma^{jk}])[{}_rG_{\phi}^{jk}]\}$$

with $[{}_rH_{\phi\phi}^c]$ and $[{}_rH_{\phi\phi}^{jk}]$ the associated centroidal and rotational Hessians of link jk, respectively. The operator "o" denotes the generalized scalar dot product [6].

Now, employing the principle of virtual work, the open-chain dynamics can be directly incorporated into closed chain dynamics according to

$$T_{\phi}^T \delta\phi = T_a^T \delta\phi_a \quad (35)$$

The total system dynamics is obtained using Eqs. (25) and (32) as follows :

$$T_a^* = [G_a^{\phi}]^T T_{\phi}$$
$$= \sum_{r=1}^{2} [{}_rG_a^{\phi}]^T([{}_rI_{\phi\phi}^*]\ {}_r\ddot{\phi} + {}_r\dot{\phi}^T[{}_rP_{\phi\phi\phi}^*]\ {}_r\dot{\phi}\}$$
$$= [I_{aa}^*]\ \ddot{\phi}_a + \dot{\phi}_a^T[P_{aaa}^*]\ \dot{\phi}_a \quad (36)$$

where the inertial matrix $[I_{aa}^*]$ and inertia power array $[P_{aaa}^*]$ defined in the independent joint set are given by

$$[I_{aa}^*] = \sum_{r=1}^{2} [{}_rG_a^{\phi}]^T[{}_rI_{\phi\phi}^*][{}_rG_a^{\phi}] \quad (37)$$

and

$$[P_{aaa}^*] = \sum_{r=1}^{2} (([{}_rG_a^{\phi}]^T[{}_rI_{\phi\phi}^*]) \cdot [{}_rH_{aa}^{\phi}] \quad (38)$$
$$+ [{}_rG_a^{\phi}]^T([{}_rG_a^{\phi}]^T \cdot [{}_rP_{\phi\phi\phi}^*])[{}_rG_a^{\phi}]\},$$

and $[{}_rG_a^{\phi}]$ and $[{}_rH_{aa}^{\phi}]$, respectively, denote the first-order and the second-order kinematic influence coefficient matrices relating the joints of ith serial chain to the whole joints of the system. If the two joints of the left open-chain of the 5-bar mechanism are chosen as the active joints, we have

$$[{}_1G_a^{\phi}] = \begin{bmatrix} 1 & 0 \\ [G_a^{\phi}]_1 \end{bmatrix}_{2\times 2}, \quad (39)$$

$$[{}_2G_a^{\phi}] = \begin{bmatrix} 0 & 1 \\ [G_a^{\phi}]_{2,3} \end{bmatrix}_{3\times 2}, \quad (40)$$

$$[{}_1H_{aa}^{\phi}]_1 = [0]_{2\times 2}\quad [{}_1H_{aa}^{\phi}]_2 = [H_{aa}^{\phi}]_1, \quad (41)$$
$$[{}_2H_{aa}^{\phi}]_1 = [0]_{2\times 2},\ [{}_2H_{aa}^{\phi}]_2 = [H_{aa}^{\phi}]_2,$$

and

$$[{}_2H_{aa}^{\phi}]_3 = [H_{aa}^{\phi}]_3. \quad (42)$$

where $[G_a^{\phi}]_1$ denotes the first row of $[G_a^{\phi}]$ and $[H_{aa}^{\phi}]_3$ denotes the first plane of the three-dimensional array $[H_{aa}^{\phi}]$. The subscriptions 1, 2 lying on the left-side of G and H represent the left and right open-chain, respectively.

Now, the dynamic formulation with respect to the output(task or operational) coordinates is obtained by employing the coordinate transformation technique between the minimum coordinates and the task coordinates :

$$T_u = [I_{uu}^*]\ \ddot{u} + \dot{u}^T[P_{uuu}^*]\ \dot{u}, \quad (43)$$

where

$$[I_{uu}^*] = [G_u^a]^T[I_{aa}][G_u^a] \quad (44)$$

and

$$[P_{uuu}^*] = [G_u^a]^T([G_u^a]^T o [P_{aaa}])[G_u^a] + ([G_u^a]^T[I_{aa}]) o [H_{uu}^a]. \quad (45)$$

T_u denotes the load vector at the output position, and

$[\Gamma_{uu}]$, $[P^*_{uuu}]$ represent the inertial matrix, inertia power array, respectively, defined in the output position.

3. Analysis on Maximum Load Handling Capacity

3.1 Maximum Load Handling Capacity

Maximum load handling capacity is defined as the maximum load that can be applied to the end-effector in any direction without exceeding any one actuator limit. Methodology to be described in the following is based on Thomas, et.al. [2]. We extend their algorithm to the case with redundant actuation.

When a given closed-chain mechanism is redundantly actuated, the actuated joint set can be described by

$$\theta_A = [\theta_s^T,\ \theta_a^T]^T \tag{46}$$

where θ_s denotes a subset of the dependent (or redundantly actuated) joint set θ_p.

The static relationship between T_u and T_A is given by

$$T_u = [G_u^A]^T T_A \tag{47}$$

where $[G_u^A]$ is equivalent to

$$[G_u^A] = [G_a^A][G_u^a]. \tag{48}$$

In Eq. (49), $[G_a^A]$ is a subset of $[G_a^\phi]$ defined in Eq. (25) and $[G_u^a]$ is the inverse of $[G_a^u]$ defined in Eq. (29). Since $[G_u^A]$ is not a square matrix and the dimension of T_A is greater than that of T_u, T_A has infinite solution for a given T_u. In particular, we employ a solution which minimize the norm $\| T_A \|$. The solution is given by

$$T_A = ([G_u^A]^T)^+ T_u \tag{49}$$

where $([G_u^A]^T)^+$ given by

$$([G_u^A]^T)^+ = [G_u^A]([G_u^A]^T[G_u^A])^{-1} \tag{50}$$

denotes the pseudo-inverse of the matrix $([G_u^A]^T)$. The limit on the driving force T_{An} at the nth actuated joint is given as

$$(T_{An})_{\min} = -T_{An}^A + T_{An}^G \tag{51}$$

and

$$(T_{An})_{\max} = T_{An}^A + T_{An}^G \tag{52}$$

where T_{An}^A is the actuation limit at the nth actuator and T_{An}^G is the gravity load at the nth actuated joint. The relationship between T_{An} and T_u is obtained from Eq. (49) as

$$T_{An} = [G_A^u]_n^T T_u \tag{53}$$

where $[G_A^u]$ is identical to $([G_u^A]^T)^+$, and $[G_A^u]_n$ denotes the *nth* column vector of $[G_A^u]$.

Now, we want T_u which simultaneously satisfies the constraint equations (51) and (52) and minimize $\| T_u \|^2$, defined as

$$\| T_u \|^2 = T_u^T [W] T_u, \tag{54}$$

where $[W] \equiv \mathrm{diag}\{W_i\}$. Lagrangian of this optimization problem having constraints is given by

$$L = \| T_u \|^2 + 2x(T_{An}), \tag{55}$$

where x is a Lagrange Multiplier. Differentiating L with respect to T_u yields

$$[W] T_u + x[G_A^u]_n = 0 \tag{56}$$

and combining Eqs. (51), (52), and (53) results in the following equation

$$(T_{An})_{ext} = [G_A^u]_n^T T_u, \tag{57}$$

where $(T_{An})_{ext}$ denotes either $(T_{An})_{\min}$ or $(T_{An})_{\max}$. Premultiplying T_u^T to both sides of Eq. (56) gives

$$\| T_u \|^2 = -x(T_{An})_{ext}. \tag{58}$$

Thus, maximum allowable load is defined as

$$\{\| T_u \|^2\}_{\max}^n = \min\{-x_a(T_{An})_{\min},\ -x_b(T_{An})_{\max}\} \tag{59}$$

where x_a, x_b denote the solution of x. After combining Eqs. (53) and (56) in a matrix form, given by

$$\begin{bmatrix} [W] & [G_A^u]_n \\ [G_A^u]_n^T & 0 \end{bmatrix} \begin{pmatrix} T_u \\ x \end{pmatrix} = \begin{pmatrix} 0 \\ (T_{An})_{ext} \end{pmatrix}, \tag{60}$$

the solution of x is obtained as

$$x = -(T_{An})_{ext}\{\sum_{j=1}^{2}([G_A^u]_{jn})^2 / W_j^2\}. \tag{61}$$

where $[G_A^u]_{jn}$ denotes the (j, n) element of $[G_A^u]$. Then, maximum load handling capacity is obtained by substituting Eq. (61) into Eq. (59)

$$(T_u)_{\max}^n = \tag{62}$$

$$\left(\sum_{j=1}^{2}\frac{([G_A^u]_{jn})^2}{W_j^2}\right)^{-\frac{1}{2}} \min\{|(T_{An})_{\min}|,\ |(T_{An})_{\max}|\}.$$

$(T_u)_{\max}^n$ should be obtained for all available actuators. Then, the smallest values among all $(T_u)_{\max}^n$ is regarded as the maximum load handling capacity.

3.2 Simulation

It is recalled that two actuators are minimally required to control the 5-bar mechanism. Here, we are concerned about where to locate the two actuators. In fact, 10 possible sets exist since there are 5 joints in the system. So far, the base joints have been preferred as the actuator location since dynamic effect due to the floating actuator can be ignored. However, the choice of the two base joints as the actuator location does not always assures the best kinematic characteristics such as manipulability and isotropy. Other set of the actuators may yield a better kinematic characteristics. Even, the dynamic effect due to the floating actuators can be discarded by using a belt system which connects the floating joint to another actuator located at the base. Therefore, in the following work, we ignore the additional dynamic effect due to the floating actuators.

We deal with the analysis of a planar 5-bar mechanism without consideration of gravity loads of the system, though it can be easily included in our problem.

Initially, the kinematic and dynamic parameters of the system are given as

$$l_1 = l_3 = l_4 = l_5 = a = 0.1m, \quad l_2 = 0.2\ m \quad (63)$$

$$m_1 = m_3 = m_4 = 0.3\ kg, \quad m_2 = 0.6\ kg$$

and

$$I_{z1} = I_{z3} = I_{z4} = 0.00025\ kg \cdot m, \quad I_{z2} = 0.002 kg \cdot m.$$

In the simulation, we measure and compare the performance of the system in terms of maximum load handling capacity. Following three issues are to be investigated :

1. Where are the best locations for the minimum actuators (2)?
2. How does one additional actuator affect the performance and where to locate it?
3. How does more additional actuators affect the performance?.

First of all, we are concerned about where to locate the minimum actuators. Assume that the maximum actuator size is given by $-1 \le T_{A_i} \le 1\ (N \cdot m)$ for each actuator. Among 10 possible minimum sets, we just compare the performances of two minimum sets $(\theta_1\ \theta_3)$ and $(\theta_1\ \theta_2)$. The desired workspace is given as $0.1 \le x,\ y \le 2.5$, as shown in Fig. 1. The curves A and B in Fig. 2 denote the distribution of maximum load handling capacity at the end-effector and it's averaged values for the minimum set $(\theta_1\ \theta_3)$ and the minimum set $(\theta_1\ \theta_2)$, respectively. The horizontal axis denotes the value of maximum load handling capacity and the vertical axis denotes the area occupied by each load handling capacity. The simulation result shows that the minimum set with one floating joint has greater load handling capacity in comparison with the maximum load handling capacity of the two base actuators.

Secondly, we are interested in the performance enhancement due to one additional actuator. The curves, C and D represent the distribution of maximum load handling capacity at the end-effector and the average value, for the actuator set $(\theta_1\ \theta_2\ \theta_3)$ and the actuator set $(\theta_1\ \theta_2\ \theta_4)$, respectively. When we compare the averaged the load handling capacity of $(\theta_1\ \theta_3)$ with that of $(\theta_1\ \theta_2\ \theta_4)$, the load handling capacity of the latter is three-times of that of the former. Though there are many possible sets with one additional actuator, the above result addresses that one additional actuator greatly improves the performance of the system, and thus the location of the additional actuator is also significant.

Thirdly, the curve E of Fig. 2 denotes the distribution of maximum load handling capacity at the end-effector and the average value when employing the whole actuators. It is observed that the load handling capacity is not much improved in comparison with that of the curve C for the case of one additional actuator. Thus, we can conclude that one additional actuator rather than many redundant actuators plays an important role in performance enhancement of the system.

4. Internal Force Applications

4.1 Feedforward Stiffness Modulation

In a state of static equilibrium, Eq. (25) can be described by

$$T_a^* = T_a + [G_a^s]^T T_s = [G_a^A]^T T_A = 0 \quad (64)$$

where

$$[G_a^A] = \begin{bmatrix} [I]_{2\times 2} \\ [G_a^s] \end{bmatrix}. \quad (65)$$

Given a disturbance to the system under force equilibrium, a spring-like behaviour occurs to the system. Assuming that the magnitude of T_A remains constant, the effective stiffness matrix $[K_{aa}]$ with respect to the independent coordinates is obtained by differentiating Eq. (64) with respect to the independent coordinate set ϕ_a[1] :

$$[K_{aa}] = (-T_A)^T o [H_{aa}^A]^T. \quad (66)$$

Noting that the stiffness relationship between the output coordinates and the independent coordinates is given by

$$[K_{uu}] = [G_u^a]^T [K_{aa}][G_u^a], \quad (67)$$

substituting Eq. (66) into Eq. (67) yields the following stiffness matrix expressed with respect to the output space

$$[K_{uu}] = (-T_A)^T o [H_{uu}^A], \quad (68)$$

where

$$[H_{uu}^A] = [G_u^a]^T [H_{aa}^A][G_u^a]. \quad (69)$$

An alternative form of Eq. (68) is given in a matrix form described by

$$K_u = -[H_u^A]\, T_A, \quad (70)$$

where K_u consist of the upper diagonal elements of $[K_{uu}]$ and $[H_u^A]$ is also obtained by collecting the upper diagonal columns of the three-dimensional array $[H_{uu}^A]$, which are defined as follow :

$$K_u = (K_{xx}\ K_{xy}\ K_{yy})^T, \quad (71)$$

$$[H_u^A] = \begin{bmatrix} ([G_u^a]^T [H_{aa}^A][G_u^a])_{xx} \\ ([G_u^a]^T [H_{aa}^A][G_u^a])_{xy} \\ ([G_u^a]^T [H_{aa}^A][G_u^a])_{yy} \end{bmatrix}. \quad (72)$$

4.2 Feedforward Frequency Modulation

Given a small displacement to the system in a state of static equilibrium $(\dot{u} = 0)$, the dynamic equation of the system is given, from Eq. (43), as

$$[I_{uu}^*]\, \delta \ddot{u} = T_u, \quad (73)$$

where

$$T_u = \Delta([G_u^A]^T T_A) = (T_A^T o [H_{uu}^A]^T)\delta u \quad (74)$$

The above equation is rearranged as

$$[I_{uu}^*]\delta \ddot{u} + [K_{uu}]\delta u = 0, \quad (75)$$

where $[K_{uu}]$ is the stiffness matrix given in Eq. (68). Premultiplying $[I_{uu}^*]^{-1}$ to both sides of Eq. (75) yields

$$\delta \ddot{u} + [I_{uu}^*]^{-1}[K_{uu}]\delta u = 0, \quad (76)$$

where the frequency matrix $[w_{uu}]$ is defined according to

$$[w_{uu}][w_{uu}]^T = [I_{uu}^*]^{-1}[K_{uu}] \quad (77)$$
$$= (-T_A)^T o([I_{uu}^*]^{-1}[H_{uu}^A]).$$

Assuming that the frequency matrix is diagonal, Eq. (77) can be written in a matrix form

$$w_u = [W_u^A]T_A, \quad (78)$$

where w_u and $[W_u^A]$ are defined as

$$w_u = (w_{xx}^2 \quad w_{xy}^2 \quad w_{yy}^2)^T \quad (79)$$

and $[W_u^A]$ is defined similar to Eq. (72).

4.3 Load Distribution Algorithms

In order to modulate the desired $[K_{uu}]$ in static equilibrium, a load distribution method is introduced in this section. Initially, combine Eqs. (64) and (70) in a matrix form, given by

$$\begin{bmatrix} [G_a^A]^T \\ -[H_u^A] \end{bmatrix} T_A = \begin{bmatrix} 0 \\ K_u \end{bmatrix}. \quad (80)$$

Then, the general solution of Eq. (80) is described by

$$T_A = [G_{com}]^+ a + ([I] - [G_{com}]^+[G_{com}])\varepsilon, \quad (81)$$

where $[G_{com}]^+$ denotes a pseudo-inverse solution of $[G_{com}]$, and $[G_{com}]$ and a are given as

$$[G_{com}] = \begin{bmatrix} [G_a^A]^T \\ -[H_u^A] \end{bmatrix}, \qquad a = \begin{bmatrix} 0 \\ K_u \end{bmatrix}. \quad (82)$$

Also, the second-term of Eq. (81) represents a homogeneous solution which creates an internal loading. This internal loading can be utilized for additional subtasks. In order to modulate a desired $[w_{uu}]$ using redundant actuation, we just need to replace $[H_u^A]$ with $[W_u^A]$ in the stiffness formulation.

4.4 Simulation

Yi와 Freeman[1] derived necessary conditions for stiffness modulation by antagonistic preloading in redundantly actuated systems. According to those conditions, a planar closed-chain system having one closed-loop has two nonholonomic constraint equations, which allow modulation of the same number of stiffness elements. Since the dimension of the matrix $[K_{uu}]$ is 2×2, only two components out of k_{xx}, k_{xy}, and k_{yy} can be independently controlled with the remaining one controlled dependently. In regard of the number of actuators, at least, four actuators are necessary to control the motion in the x- and y-directions and the magnitudes of two stiffness elements.

In simulation, the magnitudes of k_{yy} and k_{xy} are to be controlled as $0\ N/m$ and $500\ N/m$, respectively, at the position of $(x, y) = (0.1, 0.1)m$. The actuator load T_A is decided such that the desired stiffness can be modulated. In order to test the spring effect created by antagonistic redundant actuation, an initial displacement from the equilibrium position is given to the y direction by 1cm, which initiates the acceleration of the system. A fourth-order Runge-Kutta integration algorithm are used to obtain the dynamic response of the system. Fig.3 demonstrates the vibration phenomenon of the system along the y-direction. A small vibration occurs in the x-direction. This is due to the dynamic coupling between the two translational directions in the output space.

In the meanwhile, for the purpose of controlling the natural frequency of the system, we employ the frequency modulation algorithm introduced in section 4.3. The initial displacement from the equilibrium position is given the same. The actuator load T_A is decided such that ω_{xy} becomes zero and ω_{yy} is modulated as a certain value. Fig. 4 and Fig. 5 show the vibration behaviors when the natural frequencies in the y-direction are modulated as $4\ rad/\sec$ and $8\ rad/\sec$, respectively, by using redundant actuation. Since the frequency of the system is related to the period of vibration, described by

$$T = \frac{2\pi}{\omega}, \quad (83)$$

T can be estimated for each case. Just as expected, T of Fig. 4 is two times of that of Fig. 5. It is remarked that stiffness and frequency modulations will be useful in several complex assembly applications. For example, consider a two fingered hands grasping a common object. Each finger is made as our proposed 5-bar finger mechanism. It is expected that a certain assembly work such as peg-in-hole problem can be easily performed by inducing vibration to the grasped object. This vibration can be created by a synchronized motion frequency modulation of the two fingered hands. Besides assembly works, the applications of stiffness and motion frequency modulation will be diverse, which will be a future research topic.

5. Conclusions

A redundantly actuated 5-bar mechanisms is studied in this work. Judicial choice of one additional actuator greatly enhance the maximum load handling capacity of the system. The results can be applied to general closed-chain systems having redundant actuators. Furthermore, stiffness and frequency control algorithms utilizing internal loading created by redundant actuation of the system are introduced. The concept of the frequency modulation is considered fairly new. Possible applications of this concept are to be further investigated.

References

[1] Yi, B-J. and Freeman, R. A., Geometric analysis of antagonistic stiffness in redundantly actuated parallel mechanisms. *Special Issues on Parallel Closed-Chain Mechanism, Journal of Robotic systems*, Vol. 10, pp. 581-603 (1993).

[2] Thomas, M., Yuan-Chou, H.C., and Tesar, D.,

"Optimal Actuator Sizing for Robotic Manipulators Based on Local Dynamic Criteria", *ASME J. Mechnisms, Transmissions, and Auto.*, **Vol. 107**, pp. 163-169, (1985).
[3] Nakamura, Y. and Ghodoussi, M., Dynamic computation of closed-link robot mechanisms with nonredundant and redundant actuators. *IEEE Journal of Robotics and Automation*, **Vol. 5**, pp. 294-302 (1989).
[4] Kumar, V. J. and Gardner, J., Kinematics of redundantly actuated closed chain. *IEEE Journal of Robotics and Automation*, **Vol. 6**, pp. 269-273 (1990).
[5] Kurz, R. and Hayward, W., Multiple-goal kinematic optimization of a parallel spherical mechanism with actuator redundancy. *IEEE Journal of Robotics and Automation*, **Vol. 8**, pp. 644-651 (1992).
[6] R. A. Freeman and D. Tesar, Dynamic Modeling of Serial and Parallel Mechanisms/Robotic Systems, Part I-Methodology, Part II-Applications, Proc. of 20th ASME Mechanisms Conference, Orlando, FL, (1988).
[7] Asada, H. and Youcep-Toumi, K., Analyis and Design of A Direct Drive Arm with A Five-Bar Link Parallel Drive Mechanism, ASME J. of Dynamic Systems, Measurement, And Control, **Vol. 106**, **No. 3**, (1982).

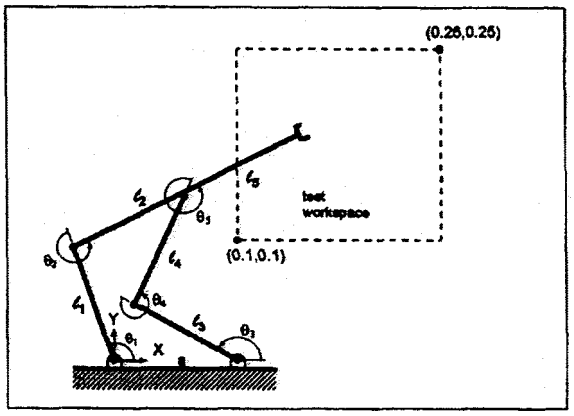

Figure 1. 5-bar Finger Mechanism

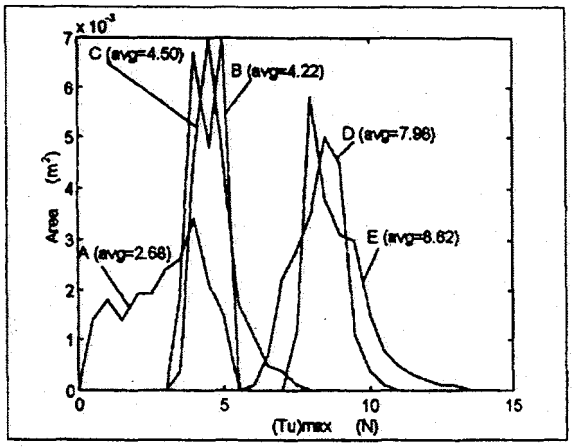

Figure 2. Maximum Load Handling Capacity

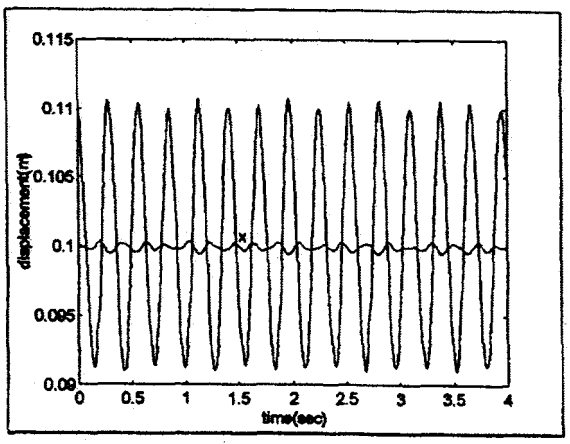

Figure 3. Spring Effect ($K_{yy} = 500N/m$)

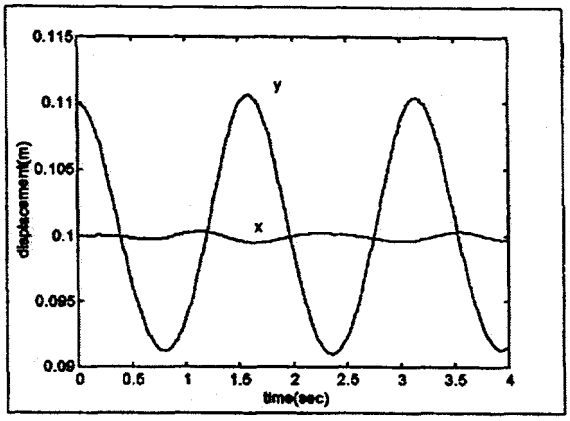

Figure 4. Frequency Control($\omega_{yy} = 4\,rad/\sec$)

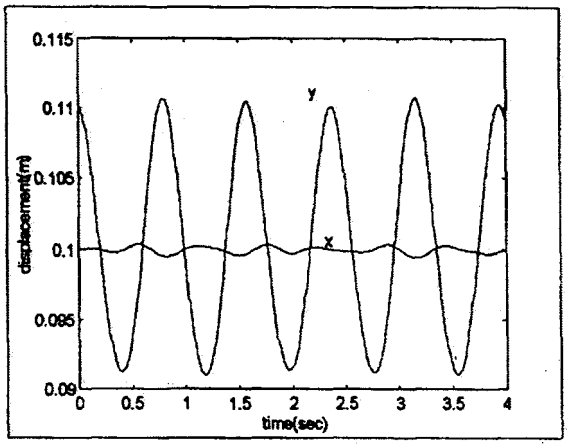

Figure 5. Frequency Control($\omega_{yy} = 8\,rad/\sec$)